energy&fuels

Article

Cite This: Energy Fuels 2018, 32, 7752−7761

pubs.acs.org/EF

Compositional and Structural Analysis of Silica Gel Fractions from Municipal Waste Pyrolysis Oils

Rebecca L. Ware,[†] Steven M. Rowland,[‡,§] Jie Lu,[§] Ryan P. Rodgers,[‡,§] and Alan G. Marshall*[,†,‡]

[†]Department of Chemistry and Biochemistry, Florida State University, 95 Chieftain Way ,Tallahassee, Florida 32306, United States

[‡]Ion Cyclotron Resonance Program, National High Magnetic Field Laboratory, Florida State University, Tallahassee, Florida 32310, United States

[§]Future Fuels Institute, Florida State University, Tallahassee, Florida 32310, United States

ABSTRACT: Hydrocarbon-rich pyrolysis oils produced from landfill waste and recycled plastics are potential sources for fuels and chemicals. It is well established that feedstock composition significantly affects pyrolysis oil composition and, hence, its potential uses. For example, plastics waste pyrolysis oils contain a high concentration of hydrocarbons, whereas biomass pyrolysis oils have high oxygen content. Previous studies have shown that the addition of plastics to a biomass feedstock increases the hydrocarbon content; however, a detailed analysis of hydrocarbons and polar species from pyrolysis oils produced from "real world" mixed municipal waste materials has not yet been done. Here, the silica gel fractions from unsorted landfill waste and mixed recycled plastics pyrolysis oils are analyzed by two-dimensional gas chromatography (GC × GC), field ionization mass spectrometry (FI-MS), Fourier transform infrared spectroscopy (FT-IR), and Fourier transform ion cyclotron resonance mass spectrometry (FT-ICR MS). Gravimetric results show that the plastics pyrolysis oil has a much greater concentration of saturated hydrocarbons than the more aromatic landfill pyrolysis oil. GC × GC and FI-MS for the saturated hydrocarbons show a range of alkanes, cycloalkanes, olefins, and 1-ring aromatics. Molecular elemental compositions from FT-ICR MS were correlated with structural assignments from GC × GC to expand the structural understanding of the aromatic hydrocarbons from plastics and landfill pyrolysis oils and showed that the aromatic hydrocarbons from the landfill are both peri- and cata-condensed. In contrast, plastics pyrolysis oil consists of polyphenyls and cata-condensed aromatic hydrocarbons. The polar species from the plastics pyrolysis oil contain more alcohol functionalities than the landfill pyrolysis oil, which contains non-carboxyl carbonyl functional groups. Improved structural understanding of both pyrolysis oils will provide better understanding of their properties and potential uses.

INTRODUCTION

Pyrolysis oils derived from waste materials are important sources of fuel and chemicals that both circumvent some of the environmental concerns associated with petroleum and alleviate waste disposal concerns. A wide range of organic waste materials, such as forestry residue and recycled plastics, may be used for pyrolysis, each producing a complex oil product with attributes governed by their chemical composition.[1−10] As for other complex mixtures, such as petroleum and dissolved organic matter, pyrolysis oils contain thousands of distinct molecular formulas.[11,12] Fractionation simplifies these samples, allowing for more detailed chemical characterization, which provides a better understanding of bulk properties and potential applications. Previous pyrolysis oil fractionation methods have focused on the separation of oxygenated species from biomass pyrolysis oils, whereas analysis of municipal waste pyrolysis oils has largely been conducted without separation.

A widely used sequential extraction that takes advantage of the range of solubilities of biomass pyrolysis oil components was proposed by Sipilä and co-workers[13] and was modified by Oasmaa and co-workers.[14−20] This extraction starts with removal of the extractives (*n*-hexane-solubles) followed by fractionation of the remaining liquid into water-solubles (aqueous phase) and water-insolubles (organic phase). The aqueous phase is further extracted with ether to obtain aldehydes, ketones, and lignin monomers (ether-solubles), as well as anhydrosugars, anhydrooligomers, and hydroxy acids (ether-insolubles). The organic phase is extracted with dichloromethane to yield low (solubles) and high (insolubles) molecular weight lignin. This method is beneficial for characterization of phase separations, acidity, and storage stability of biomass pyrolysis oils; however, there is extensive coextraction of nonpolar compounds as well as competition between polar compounds. The coextraction of nonpolar compounds results in the need for further extractions to recover specific value-added chemicals.[21] Fu and co-workers[22] successfully concentrated phenols from a lignin-derived pyrolysis oil by extraction with a switchable hydrophilicity solvent. However, that method also suffers from carryover. Solvent extractions such as these require components with large differences in solubility (e.g., hydrophobic versus hydrophilic) and are not applicable to hydrocarbon-rich municipal waste pyrolysis oils.

A fractionation method for pyrolysis oils based on functionality, similar to a petroleum SARA fractionation,[23] was developed by Pütün and co-workers.[24,25] In that method, a heptane extraction is followed by elution with pentane, toluene, ether, and methanol from a silica gel column, resulting in four fractions: heptane-insolubles, saturated and aromatic hydro-

Received: February 16, 2018
Revised: May 31, 2018
Published: June 20, 2018

DOI: 10.1021/acs.energyfuels.8b00596
Energy Fuels 2018, 32, 7752−7761

carbons, and polar species. As with separations for biomass-derived pyrolysis oils, that method has limited application to municipal waste pyrolysis oils because it targets polar, oxygenated compounds. A similar silica gel extraction was applied to a variety of biomass and plastics model compounds by Zhou and co-workers,[7] specifically for isolation and characterization of polyaromatic hydrocarbons (PAHs). Their analysis showed that plastic materials produce more PAHs than biomass; however, it was limited in its understanding of mixed waste feedstocks and PAHs with >4 aromatic rings. A different silica gel fractionation was conducted by Toraman and co-workers[26] to isolate and analyze nitrogen- and sulfur-containing compounds from a plastics solid waste pyrolysis oil. That method successfully removed interferences from hydrocarbon species (91% determined by GC) to allow for accurate analysis of low-abundance nitrogen (1.08 wt %) and sulfur (0.17 wt %) species. Although several studies, including those utilizing chromatographic fractionations, have investigated the composition of pyrolysis oils from individual municipal solid waste streams, little information is available for mixed waste streams.

It is important to have appropriate analysis in conjunction with separations, with the best analysis techniques determined by the sample. However, for complete composition coverage of all species in a complex mixture, multiple analyses are required. Common analysis methods for pyrolysis oils are infrared spectroscopy (IR),[4,5,24,25,27−30] flame ionization detectors (FID), and mass spectrometers; the latter two are often coupled with gas chromatography (GC).[5−8,13,16,20,21,24−29,31−44] With these methods, it has been shown that plastics pyrolysis oils are composed mainly of alkanes, aromatic compounds, and a small amount oxygen-containing species (<2 wt % by elemental analysis).[26,30,38,44,45] Much of the current research has focused on characterization of individual plastic feedstocks rather than feedstocks mixed with other plastics or biomass.[9,10] When biomass is mixed with plastics in the form of municipal solid waste, the characterization becomes more difficult because of the more complex nature of the oil. Those samples display characteristics of both biomass and plastics pyrolysis products; illustrated by a high oxygen content along with an increased concentration of alkanes.[5−8] Fourier transform ion cyclotron resonance (FT-ICR) mass spectrometry (MS) has proven essential for the analysis of nonvolatile, polar species that are not detected by GC, such as large PAHs and oxygen-containing species.[11,12,16,46−49] Here, we couple a silica gel separation with a range of analysis methods specifically selected for extensive characterization of each sample. To gain a better understanding of their bulk properties (elemental analysis and gravimetric results), field ionization (FI) MS, comprehensive two-dimensional gas chromatography (GC × GC), Fourier transform IR (FT-IR), and FT-ICR MS are used for extensive characterization of the saturated and aromatic hydrocarbons and polar species from unsorted landfill waste and mixed recycled plastics-derived pyrolysis oils.

EXPERIMENTAL METHODS

Sample Preparation. Pyrolysis oil samples were obtained from PER North America (landfill pyrolysis oil: Duluth, GA) and GenAgain Technologies, LLC (plastics pyrolysis oil: Lithia Springs, GA). Pyrolysis and feedstock conditions are described elsewhere.[49] The landfill feedstock is unsorted and contains both biomass and nonbiomass materials. The plastic feedstock contains unsorted recycled plastics. Prior to analysis, a dry nitrogen gas (N_2) flow was used to remove the volatile components from the samples.

Bulk Properties. Bulk properties were measured at Intertek. The ASTM methods for kinematic viscosity, total acid number, and ash content were D445, D664, and D482.

Silica Gel Fractionation. Three fractions from each pyrolysis oil, consisting of the saturated and aromatic hydrocarbons and polar species were obtained from a silica gel fractionation.[49] A 10 mL glass pipet (column) was packed with 2 g of dry silica gel and conditioned with 10 mL of cyclohexane (HPLC grade, JT Baker, Phillipsburg, NJ). Approximately 20 mg of sample in 2 mL of cyclohexane was loaded onto the column and equilibrated for 15 min. Then, 20 mL of 100% cyclohexane eluted saturated hydrocarbons in the first fraction. Next, the aromatic hydrocarbons were eluted with 20 mL of a mixture of cyclohexane and DCM (90:10, v/v). Polar species were eluted in the third fraction with 10 mL of DCM/methanol (50:50, v/v) and 10 mL of methanol. All fractions were desolvated under N_2.

Bulk Elemental Analysis. Bulk elemental analysis was performed as described elsewhere with a Thermo Finnigan (San Jose, CA) elemental analyzer (Flash EA 1112).[12,49] C and H were determined with a sample mass between 1 and 2 mg. Calibration of the instrument was provided by analysis of a lubricant oil standard for C and H (CE Elantech, Lakewood, NJ). Each sample analysis sequence also included lubricant oil to ensure accuracy over time.

GC × GC-MS. Comprehensive two-dimensional gas chromatography with time-of-flight (TOF) MS detection was performed with a Leco Pegasus 4D system (Leco Corp., St. Joseph, MI) as described elsewhere.[49] The first column was a nonpolar dimethyl polysiloxane column (60 m × 0.25 mm ID, 0.25 μm film thickness, SGE, Inc.) and the second was a polar 50% phenyl polysilphenylene-siloxane column (1.4 m × 0.25 mm ID, 0.1 μm film thickness, SGE, Inc.). Then, 1 μL of a 30 mg/mL solution of each sample in dichloromethane (DCM) was injected without a split. The gas chromatograph inlet temperature was 300 °C. For the saturated hydrocarbons, the first oven temperature was set at 40 °C for 0.5 min before ramping to 340 °C at a rate of 1 °C/min. That temperature was held for 10 min. The second column was set 10 °C higher than the first and followed the same temperature increase profile. The modulator offset was +20 °C with a modulation period of 12 s and a hot pulse of 1.5 s. Parameters for the aromatic hydrocarbons were the same except that the first oven temperature was held for 4 min before ramping at a rate of 3 °C/min. The second oven was set 5 °C higher than the first, and the modulator offset was +10 °C with a modulation period of 6 s and a hot pulse of 0.8 s. The data were acquired and processed with ChromaTOF software (version 4.50) from LECO Corp. NIST libraries of model compounds were used to assign possible structures based on a similarity of >85% in the fragmentation patterns. Semi-quantitation was done by calculating the percent peak area for each region, in which the total peak area of a region was divided by the total peak area of the chromatogram then multiplied by 100.

FI-MS. Field ionization coupled with time-of-flight mass spectrometry was performed with a Waters GCT Premier instrument (Waters Corp., Milford, MA). Approximately 50 μg of saturated hydrocarbon sample was loaded into a quartz sample cup and inserted into the FI-MS solids probe. The initial temperature of the probe was 30 °C and was held for 0.1 min before ramping to 325 °C at a rate of 15 °C/min. Data were acquired with MassLynx software provided by Waters Corp, and formula assignments and imaging were done with PetroOrg software.[50]

FT-ICR MS. Samples were dissolved in toluene (hydrocarbons) or a 50:50 mix of toluene and methanol (polar species) to a concentration of 1 mg/mL. Further dilution to 100 μg/mL in toluene (HPLC grade, JT Baker, Phillipsburg, NJ) was done for positive-ion (+) atmospheric pressure photoionization (APPI) analysis. Toluene was used as the APPI solvent to promote photoionization. A custom built 9.4 T FT-ICR mass spectrometer was used for FT-ICR MS analysis and is described elsewhere.[47,51−53] A Thermo Scientific APPI source generated ions and was equipped with a Krypton lamp that emits 10.0 and 10.6 eV photons, a nebulizer with a temperature of 300 °C, sheath gas of 60 p.s.i., an auxiliary gas flow of ∼4 L/min, and a sample

DOI: 10.1021/acs.energyfuels.8b00596
Energy Fuels 2018, 32, 7752−7761

flow rate of 50 μL/min. Fifty ~4.6 s time-domain transients were co-added for each spectrum. Mass spectral calibration, formula assignments, and imaging were conducted with PetroOrg software.[50,52]

FT-IR. A PerkinElmer Spectrum 100 ATR FT-IR spectrometer was used for infrared analysis. The zinc selenide crystal was covered with a sufficient amount of sample and scanned over the 4000−500 cm^{-1} frequency range.

RESULTS AND DISCUSSION

Gravimetric results from the silica gel fractionation (Table 1) show a high concentration of saturated hydrocarbons in the plastics pyrolysis oil and greater concentration of aromatic hydrocarbons and polar species in the landfill pyrolysis oil, likely due to plant and food material in the landfill feedstock. H/C ratios calculated from elemental analysis indicate that the plastics saturated hydrocarbons (H/C = 2.0) are composed of a greater concentration of straight-chain and branched alkanes than the saturated hydrocarbons from the landfill pyrolysis oil (H/C = 1.8), which contains a greater concentration of cycloalkanes and olefins. The H/C ratios for the aromatic hydrocarbons (1.5) and polar species (1.4) are the same for both pyrolysis oils; however, the amounts of aromatic and polar compounds in the landfill sample is approximately 2.3 and 3.1 times greater than those for the plastics pyrolysis oils. Mass recoveries less than 100% are due to loss of abundant volatile species during devolatilization of the fractions.

Table 1. Gravimetric Results (Mass %) and H/C Ratios for Silica Gel Fractionation of Landfill and Plastics Pyrolysis Oils

fraction	landfill		plastics	
	mass %	H/C	mass %	H/C
saturated hydrocarbons	38.5%	1.8	72.9%	2.0
aromatic hydrocarbons	16.1%	1.5	6.9%	1.5
polar species	37.1%	1.4	11.6%	1.4
total recovery	91.6%		91.3%	

Saturated Hydrocarbons. GC × GC-MS profiles of the saturated hydrocarbons from landfill and plastics pyrolysis oils show a range of linear, branched, and cycloalkanes ranging from ~C_7 to C_{27} (Figure 1). The plastics pyrolysis oil was found to have a percent peak area in the alkane region (40.9%) somewhat greater than that of landfill pyrolysis oil (36.1%) (Figure 2, outer ring). Of the identified peaks in that region of the plastics chromatogram, 28.4% are normal alkanes, 10.5% are branched alkanes, and 7.7% as cycloalkanes (Figure 2, inner circle). The alkane region of the landfill chromatogram contains 19.4% normal alkanes, 9.3% branched alkanes, and 3.3% cycloalkanes. The sub-regions of both the plastics and landfill pyrolysis oils contain a significant portion of unknown peaks, due to lack of library matches and the complexity of pyrolysis oils. The unknowns that did not fall within a region consisted of 10% and 14.6% of the peak area of the plastics and landfill pyrolysis oil chromatograms. The abundance of compounds with lower carbon numbers in the landfill pyrolysis oil is illustrated by the percent peak area for the $<C_{10}$ region, which is 6 times greater for the landfill (6.1%) than for the plastics (0.9%) (Table 2). The presence of compounds with one aromatic ring in the first fraction demonstrates incomplete separation of saturated hydrocarbons from aromatic hydrocarbons, likely due to steric hindrance of functional groups and large hydrophobic side chains on aromatic species. This incomplete separation is more pronounced in the landfill pyrolysis oil, with 15.1% in the 1-ring aromatic region. The landfill pyrolysis oil feedstock contains both biomass and plastic materials, resulting in products from both. The subtraction of the plastics chromatogram from the landfill chromatogram shows the components unique to the landfill pyrolysis oil; theoretically, species produced from biomass material in the feedstock (Figure 1, bottom). Those components include low molecular weight alkanes and aromatic species.

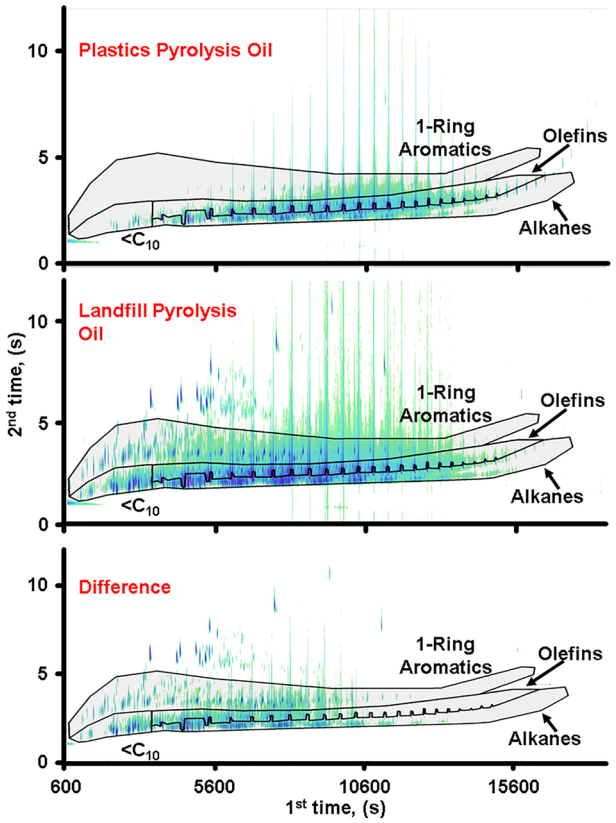

Figure 1. GC × GC-MS chromatograms for saturated hydrocarbons from plastics (top) and landfill (middle) pyrolysis oils. The bottom landfill-minus-plastics chromatogram shows components unique to the landfill pyrolysis oil. Regions for $<C_{10}$ alkanes/olefins, alkanes, olefins, and 1-ring aromatic compounds are shown.

The construction of Figure 2 deserves explanation. Because the sum of all of the peak areas must be the same, irrespective of how they are sorted, the area bounded by the outer annulus must be the same as the combined area of the inner pie slices. Let r_1 represent the radius of the outer boundary of the annulus and r_2 be the radius of the inner boundary of the annulus. Then

$$\text{area between the two circles} = \pi r_1^2 - \pi r_2^2 \quad (1)$$

$$\text{area inside the inner circle} = \pi r_2^2 \quad (2)$$

$$\text{therefore, } \pi r_1^2 - \pi r_2^2 = \pi r_2^2 \quad (3)$$

$$\text{and } r_2 = r_1/\sqrt{2} \quad (4)$$

The carbon number range for GC × GC is 7−27, which precludes the detection of large nonvolatile polar components. FI-MS provides unbiased ionization of the whole range of carbon numbers without fragmentation or oxidation in the source. Carbon number distributions derived from FI-MS (Figure 3) show a carbon range of 11−40 for the plastics

DOI: 10.1021/acs.energyfuels.8b00596
Energy Fuels 2018, 32, 7752−7761

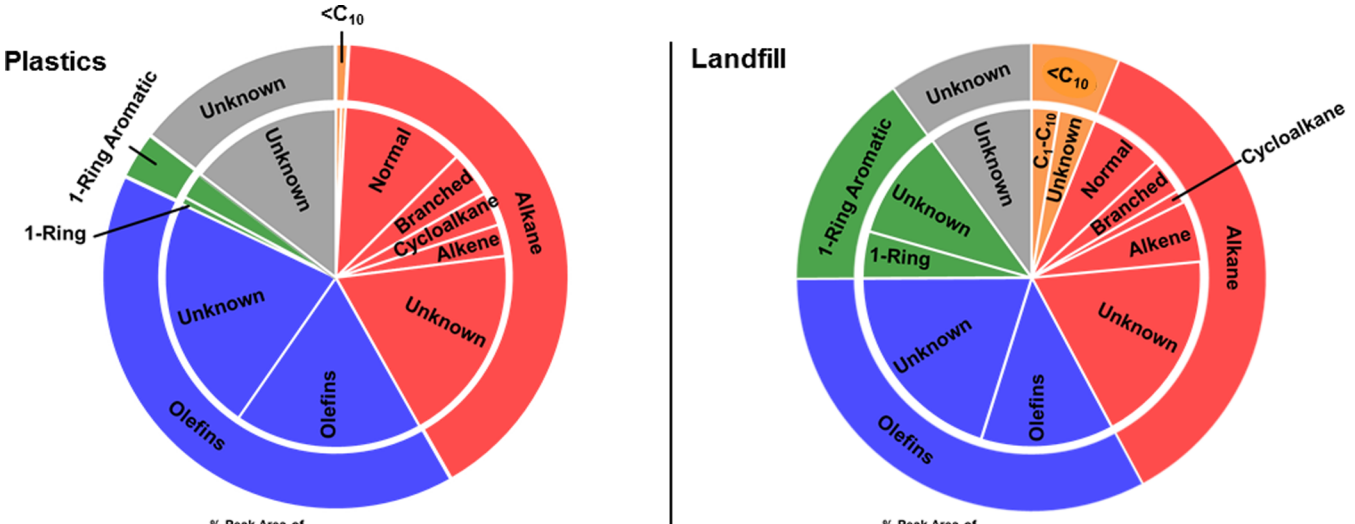

Region	% Peak Area of Chromatogram	Sub Region	% Peak Area of Region
<C10	0.9	< C10	53.0
		Unknown	47.0
Alkanes	40.9	Normal	28.4
		Branched	10.5
		Cycloalkane	7.7
		Alkene	7.2
		Unknown	46.2
Olefins	40.4	Olefins	44.2
		Unknown	55.8
1-Ring Aromatics	3.3	1-Ring Aromatics	21.6
		Unknown	78.4
Unknown	14.6	Unknown	100

Region	% Peak Area of Chromatogram	Sub Region	% Peak Area of Region
< C10	6.1	< C10	42.3
Unknown		Unknown	57.7
Alkanes	36.1	Normal	19.4
		Branched	9.3
		Cycloalkane	3.3
		Alkene	16.1
		Unknown	51.9
Olefins	32.8	Olefins	38.7
		Unknown	61.3
1-Ring Aromatics	15.1	1-Ring Aromatics	29.6
		Unknown	70.4
Unknown	10.0	Unknown	100

Figure 2. Pie charts representing the percentage of total chromatogram peak area for hydrocarbons from plastics (left) and landfill (right) samples, broken down according to alkanes/olefins/1-ring aromatic/unassigned (outer ring) and additional subcategories (inner pie chart). Because the sum of all of the peak areas must be the same, irrespective of how they are sorted, the area between the two circles is the same as the area inside the inner circle (see text).

Table 2. Percent Peak Areas for Compound Regions in the GC × GC Profiles of the Saturated and Aromatic Hydrocarbons from Plastics and Landfill Pyrolysis Oils

	Saturated Hydrocarbons	
	plastics (%)	landfill (%)
<C10	0.9	6.1
alkanes	40.9	36.1
olefins	40.4	32.8
1-ring aromatic	3.3	15.1
unassigned peaks	14.6	10.0
	Aromatic Hydrocarbons	
	plastics (%)	landfill (%)
alkanes	3.1	1.3
1-ring aromatic	20.7	15.1
2-ring aromatic	36.1	41.6
3-ring aromatic	16.5	20.3
4-ring aromatic	2.8	7.4
unassigned peaks	20.8	14.3

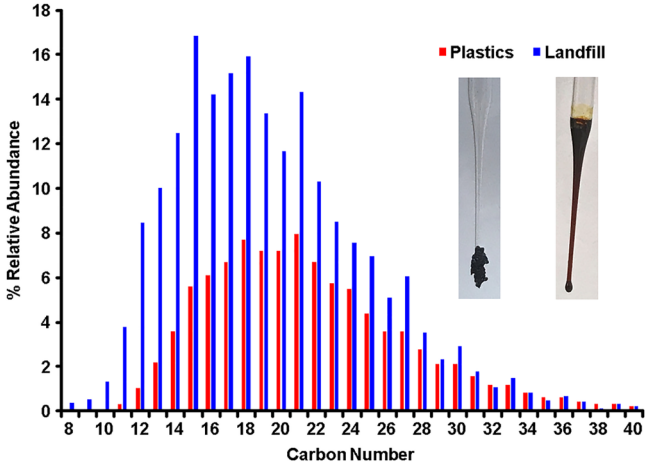

Figure 3. FI-MS-derived carbon number distributions for saturated hydrocarbons from landfill and plastics pyrolysis oils.

pyrolysis oil with an abundance-weighted average of 22 carbons, i.e., a few carbons greater than that in the landfill pyrolysis oil, which ranges from 8 to 40 with an abundance-weighted average of 19 carbons. The paraffinic nature of the plastics pyrolysis oil is due to its high concentration of saturated hydrocarbons (72.9 wt %) and high carbon number. The high concentration of paraffins in the plastics pyrolysis oil results in an elevated viscosity (10.71 mm^2/s) relative to the landfill pyrolysis oil (2.013 mm^2/s) (see images in Figure 2). FI-MS-derived double bond equivalents (DBE = number of rings plus double bonds to carbon = $c - h/2 + n/2 + 1$ for $C_cH_hN_n$...)) versus carbon number plots for the saturated hydrocarbons from landfill and plastics pyrolysis oils (Figure 4) reveal several homologous series of hydrocarbons, each having the same DBE but different number of carbons. In the plastics pyrolysis oil, the preponderance of components with low DBE (0 and 1) and high carbon numbers confirms the abundant paraffinic hydrocarbons seen by GC × GC. In addition to the predominant species at DBE 0−1, the landfill pyrolysis oil has compositional series of DBE 4 and 7, which correspond to molecules with one and two benzene rings, as also seen by GC × GC.

DOI: 10.1021/acs.energyfuels.8b00596
Energy Fuels 2018, 32, 7752−7761

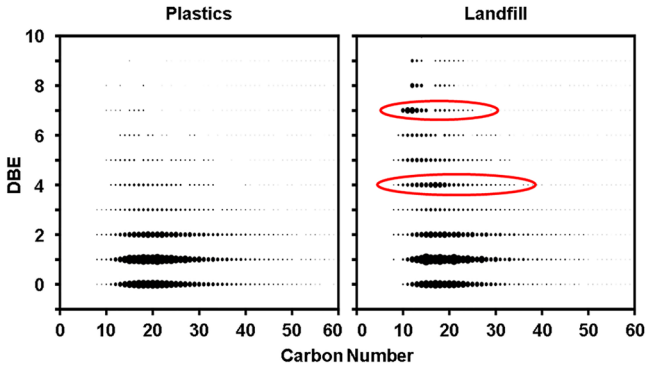

Figure 4. FI-MS-derived isoabundance-contoured plots of double bond equivalents (DBE) versus carbon number for the saturated hydrocarbons from the landfill and plastic pyrolysis oils.

Aromatic Hydrocarbons. Identification of aromatic components in pyrolysis oils is important because certain aromatic structures can cause coke deposition and toxicity, both of which increase the cost of pyrolysis oil production.[39,54] GC × GC-MS profiles of the aromatic hydrocarbons from landfill and plastics pyrolysis oils (Figure 5) show components containing between 1 and 4 aromatic rings not previously seen in GC × GC for the unfractionated pyrolysis oils.[49] Carryover of saturated hydrocarbons from the first fraction (signal below 2 s in the second dimension) is more prominent for the plastics pyrolysis oil (3.1%) than for the landfill (1.3%). Based on the percent peak area for the 1-ring aromatic species, the landfill

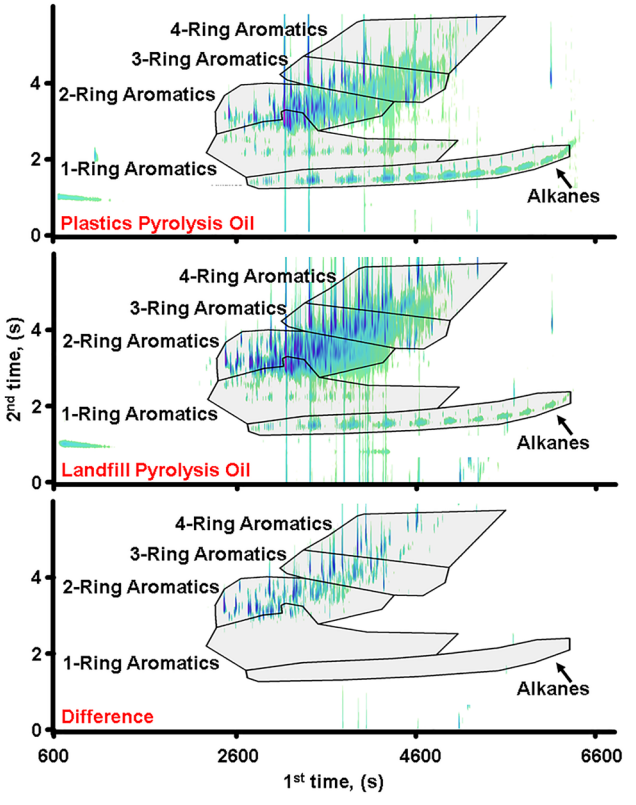

Figure 5. GC × GC-MS chromatograms for aromatic hydrocarbons from plastics (top) and landfill (middle) pyrolysis oils. The bottom landfill-minus-plastics chromatogram shows components unique to the landfill pyrolysis oil. Regions for alkanes and 1-ring through 4-ring aromatic compounds are shown.

pyrolysis oil contains fewer of these components than the plastics pyrolysis oil. However, that estimate is not accurate because of elution of 1-ring aromatic species in the saturated hydrocarbon fraction. To appropriately account for the number of components containing one aromatic ring, the percent peak area from the 1-ring aromatic region within the saturated hydrocarbons chromatogram should be added to the percent peak area from the aromatic hydrocarbons chromatogram, resulting in a total peak area of 30.2% for components containing one aromatic ring in the landfill pyrolysis oil and 24.0% for the plastics pyrolysis oil. This calculation shows, as expected, that the combined aromatic components are more abundant in the landfill pyrolysis oil (Table 2). The presence of aromatic species in greater concentration (16.1 wt %) accounts for the ash content of the landfill pyrolysis oil (0.022 wt %) compared to plastics (0.001 wt %). Ash content for the plastics and landfill pyrolysis oils is low in contrast to plant-based bio-oils that have ash contents of up to 0.2 wt %.[1] GC × GC-MS provides semi-quantitation and structural information for low molecular weight aromatic species but is limited in its characterization of large polycyclic aromatic hydrocarbons.

FT-ICR MS is advantageous for the identification of high molecular weight non-volatile species not accessed by GC × GC-MS. FT-ICR MS-derived DBE versus carbon number plots for the hydrocarbon classes from the aromatic fractions illustrate higher molecular weight aromatic species than are identified by GC × GC-MS (Figures 6 and 7). The narrow compositional coverage for landfill oil (abundance-weighted average DBE = 12, carbon number = 21) reveals the presence of heavily condensed aromatic ring structures close to the PAH line. The PAH line marks the highest degree of unsaturation possible in natural planar aromatic structures.[55,56] The broad compositional coverage for the plastics pyrolysis oil (abundance-weighted average DBE = 11, carbon number = 28) indicates the presence of aromatic species that also contain saturated rings or aliphatic moieties. Although FT-ICR MS shows compositional trends, it does not provide information about the structures responsible for these trends.

The combination of GC × GC (carbon number 5−30, DBE 0−15) and FT-ICR MS (carbon number 15 to >70 and DBE ~ 1 to >30) enables more complete coverage of carbon number and DBE ranges for both polar and nonpolar species and enables extrapolation of structural information beyond what is detectable by GC × GC-MS alone.[57] Extrapolation is done by first identifying structural series with consistently higher DBE and carbon number in the DBE versus carbon number plot. Then, molecular elemental compositions (from GC × GC-MS and FT-ICR MS) and structures (from GC × GC-MS) are correlated for species in the series that fall within the region covered by both GC × GC-MS and FT-ICR MS. Given the known structures and consistent increases in DBE and carbon number, the structural information is then extrapolated into the region of the plot that is seen only by FT-ICR MS. Specific isomers are not identified by this method; therefore, the structures shown represent selected possible isomers. The compounds in these complex samples likely constitute a mixture of many different isomers. For example, Figure 6 shows structures assigned for two selected series in the DBE versus carbon number plot for the hydrocarbon class from the landfill pyrolysis oil. In the first series, structures become more peri-condensed (contain internal carbons) with the addition of aromatic rings as carbon number and DBE increase. Series 2 (Figure 6) also shows the addition of aromatic rings; however,

DOI: 10.1021/acs.energyfuels.8b00596
Energy Fuels 2018, 32, 7752−7761

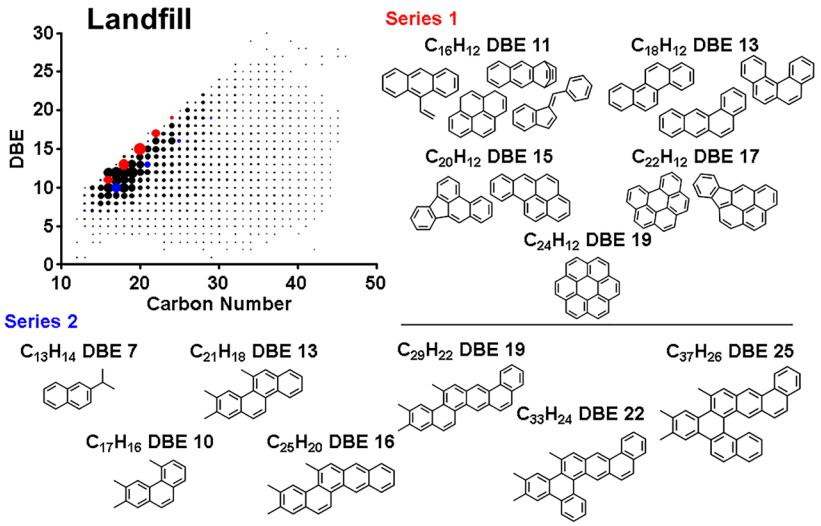

Figure 6. FT-ICR-MS-derived isoabundance-contoured plots of DBE versus carbon number for the aromatic hydrocarbons from the landfill pyrolysis oil. Peri-condensed structures are seen in series 1, whereas series 2 shows cata-condensed structures.

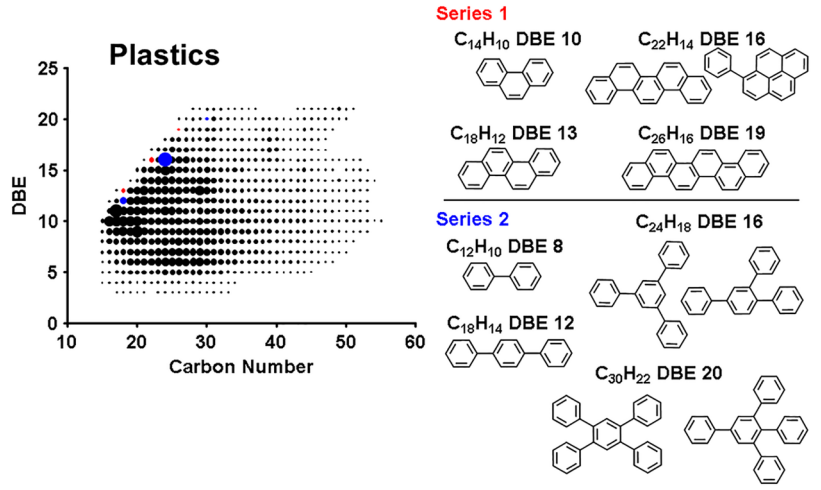

Figure 7. FT-ICR-MS-derived isoabundance-contoured plots of DBE versus carbon number for the aromatic hydrocarbons from the plastics pyrolysis oil. Cata-condensed structures are seen in series 1, whereas series 2 shows polyphenyl structures.

that series is cata-condensed (no internal carbons). In series 1, all identified compounds fall within the overlap region between GC × GC-MS and FT-ICR MS. In series 2, hypothetical structures were identified for compounds beyond what was identifiable with GC × GC-MS (carbon number > ~30), specifically, $C_{33}H_{24}$ (DBE 22) and $C_{37}H_{26}$ (DBE 25). In the DBE versus carbon number plot for the hydrocarbon class from the plastics pyrolysis oil (Figure 7), series 1 exhibits cata-condensed structures similar to those in series 2 from the landfill oil. In contrast, series 2 (Figure 7) in the plastics pyrolysis oil contains phenyl additions onto a benzene core. Large polyphenyl structures help to explain the wide range in carbon number (~15−60) in addition to a high degree of alkylated aromatic cores, in the form of alkyl chains around or between cores. For both series in the plastics pyrolysis oil, the first compound was observed only by GC × GC-MS, whereas the last compound was seen only by FT-ICR MS. Combination of GC × GC with FT-ICR MS analysis expands the structural information for these samples, to provide a more detailed characterization.

Different unit additions within compositional space can theoretically be identified by a series slope in DBE versus carbon number plots (Figure 8) to provide quick identification of structural trends.[57] The peri-condensed (PAH line) unit addition has a slope of 0.9 and is the most condensed planar carbon structure possible before corannulene and fullerenes forms.[56] Less condensed series have smaller slopes, farther from the PAH line. The green and orange lines represent cata-condensed and polyphenyl unit additions, each with a smaller slope consistent with decreasing condensation. Any addition of non-aromatic carbon would result in a much smaller slope, illustrated by a cycloalkane unit addition. In the cycloalkane series, the structural additions are saturated rings resulting in a DBE increase of one for every six carbons. The position of the cycloalkane line in the DBE versus carbon number plot makes it easy to differentiate from the other types of unit additions. The unit addition lines shown are representative structures, and actual structures could change carbon number and/or DBE. For example, a polyphenyl series with a slope of 0.7 but with a carbon number higher than that of the illustrated series could have alkyl chains on, or between, the phenyl groups. However,

DOI: 10.1021/acs.energyfuels.8b00596
Energy Fuels 2018, 32, 7752−7761

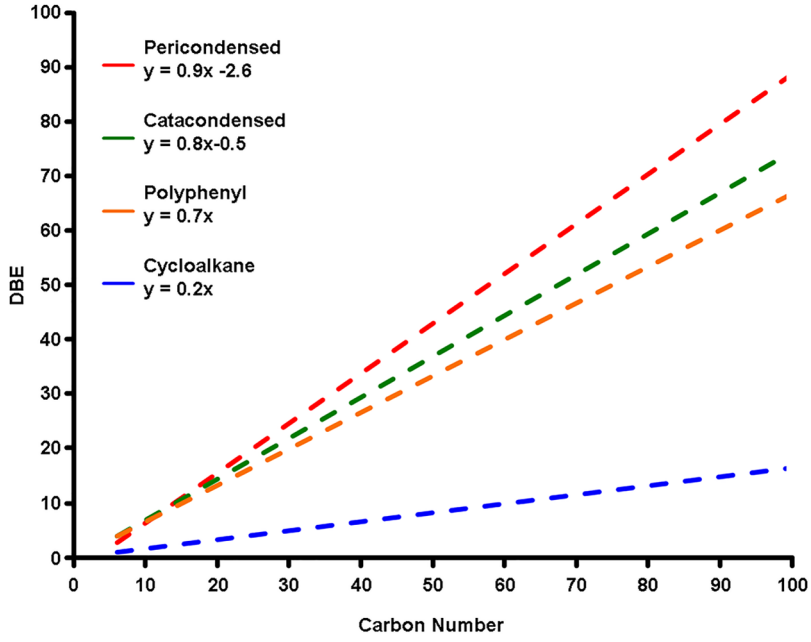

Figure 8. Unit addition trend lines for compositional coverage in FT-ICR MS-derived DBE versus carbon number plots (see text).

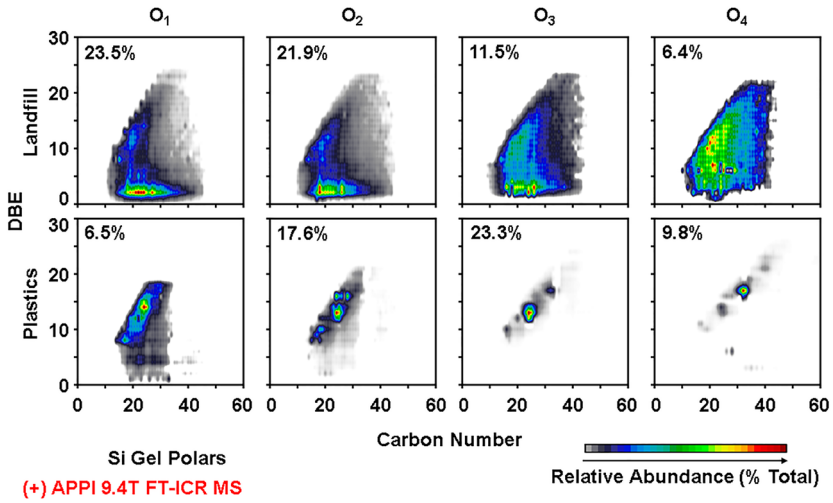

Figure 9. FT-ICR MS-derived isoabundance-contoured plots of DBE versus carbon number for the O_1–O_4 heteroatom classes from the polar species silica gel fractions from the landfill and plastics pyrolysis oil.

for the same slope as the illustrated series, the structural unit added is the same (single benzene ring). Similarly, if the series starts with naphthalene instead of benzene, the DBE would shift up 3, but with the addition of single benzene rings, the slope would still be 0.7. Compositional coverage and slope in DBE versus carbon number plots can give insight as to the types of structures (PAH versus cycloalkane); however, it is not sufficiently specific to differentiate between similar series (peri- versus cata-condensed). The slopes in Figure 8 provide compositional boundaries and angles for types of structural unit additions to better understand structural motifs.

Polar Species. The third silica gel fraction contained polar species comprised of mostly oxygen-containing compounds. The compositional coverage seen in the FT-ICR MS-derived DBE versus carbon number plots (Figure 9) for the O_1–O_4 heteroatom classes shows different trends in landfill and plastics pyrolysis oils. The plastics pyrolysis oil exhibits polar species with a range of carbon number from 15–35 and a DBE from 1–18. Oxygen species in this oil are due to alcohol groups, as shown by FT-IR absorbance at 3300 cm^{-1} (O–H stretch) and weak absorbance in the carbonyl region (1700 cm^{-1}) (Figure 10, top). The oxygen classes seen in the landfill pyrolysis oil have a bimodal distribution with carbon numbers between 10–55 and DBE from 1–25, similar to what is seen for the unfractionated landfill pyrolysis oil.[49] Those oxygen species mainly correspond to non-carboxyl carbonyl groups, as shown by the high absorbance at 1700 cm^{-1} with low absorbance at 3300 cm^{-1} (Figure 10, bottom). The effect of the polar species on bulk properties is greater for the landfill pyrolysis oil because they constitute approximately a third of the total mass (37.1 wt %), whereas plastics comprise only a tenth of the polar species (11.6 wt %). For example, the landfill pyrolysis oil has an acid number of 43 mg of KOH/g, whereas the acid number for plastics is negligible.

DOI: 10.1021/acs.energyfuels.8b00596
Energy Fuels 2018, 32, 7752–7761

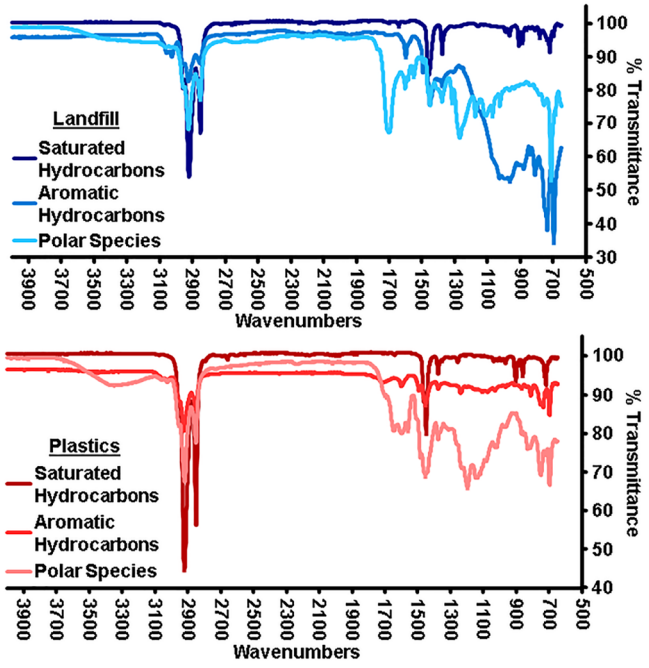

Figure 10. FT-IR spectra for the silica gel polar species fraction from landfill and plastics pyrolysis oils.

CONCLUSIONS

Herein we describe a simple silica gel fractionation method, combined with the use of a collection of analytical methods (bulk property analysis, elemental analysis, GC × GC MS, FI-MS, FT-ICR MS and FT-IR) specifically chosen to address chemical structures/functionalities known to elute in given chromatographic fractions. The approach yields a molecular level analysis that correlates with bulk property (assay-type) and elemental analyses but exposes important compositional differences between landfill- (unsorted municipal solid waste) and plastic-derived pyrolysis oils not detectable by conventional methods. Analysis of the saturate fraction by GC × GC MS confirmed the paraffinic nature of the plastic pyrolysis oil and more aromatic characteristics of the landfill oil. FI-MS was used to extend the carbon number range from ~C_{27} (GC × GC-MS) to ~C_{40} and provided semi-quantitative confirmation of the compositional trends revealed by GC × GC-MS. The approach was repeated for the aromatic fraction, with FT-ICR MS in place of FI-MS, and exposed the narrow, but more abundant, compositional space of the landfill aromatic species. Structural series identified in the GC × GC-MS analysis, combined with overlapping coverage by FT-ICR MS analysis, facilitated extension of molecular-level information beyond the GC range. Since peri- and cata-condensed structures exhibit different slopes when visualized in DBE versus carbon number space, the slope of abundant structural series provides additional compositional information. Due to the high oxygen content, the last silica gel fraction (polars) was analyzed by FT-ICR MS and FT-IR. The FT-ICR MS analysis revealed an abundant, bimodal (low and high DBE) distribution of O_x species in the landfill oil, whereas the plastic oil consisted of only the high DBE distribution. Although the high DBE distributions for the O_x species in the landfill and plastic oils occupied a similar DBE/carbon number compositional space, FT-IR data strongly suggested that the plastic O_x species were due to alcohols, whereas the landfill O_x species were predominately ketone and aldehydes (non-carboxylic carbonyls).

AUTHOR INFORMATION

Corresponding Author

*E-mail: marshall@magnet.fsu.edu. Phone: +1 850-644-0529. Fax: +1 850-644-0133.

ORCID

Ryan P. Rodgers: 0000-0003-1302-2850
Alan G. Marshall: 0000-0001-9375-2532

Notes

The authors declare no competing financial interest.

ACKNOWLEDGMENTS

The authors thank PER North America and GenAgain Technologies for providing the samples and Greg T. Blakney, Donald F. Smith, and John P. Quinn for continued assistance in instrument maintenance and data analysis. The authors also thank Yuri E. Corilo for help with FI-MS data processing and for providing data processing and imaging software. The authors gratefully acknowledge LECO Corporation for continued support with GC × GC MS. This work was supported by the NSF Division of Materials Research (DMR-1157490) and the State of Florida.

REFERENCES

(1) Mohan, D.; Pittman, C. U.; Steele, P. H. Pyrolysis of Wood/Biomass for Bio-Oil : A Critical Review. *Energy Fuels* **2006**, *20* (3), 848−889.
(2) Jahirul, M.; Rasul, M.; Chowdhury, A.; Ashwath, N. Biofuels Production through Biomass Pyrolysis —A Technological Review. *Energies* **2012**, *5*, 4952−5001.
(3) Xiu, S.; Shahbazi, A. Bio-Oil Production and Upgrading Research: A Review. *Renewable Sustainable Energy Rev.* **2012**, *16*, 4406−4414.
(4) Islam, M. N.; Islam, M. N.; Beg, M. R. A.; Islam, M. R. Pyrolytic Oil from Fixed Bed Pyrolysis of Municipal Solid Waste and Its Characterization. Renew. *Renewable Energy* **2005**, *30* (3), 413−420.
(5) Buah, W. K.; Cunliffe, a M.; Williams, P. T. Characterization of Products from the Pyrolysis of Municipal Solid Waste. *Process Saf. Environ. Prot.* **2007**, *85* (B5), 450−457.
(6) Huang, Q.; Tang, Y.; Lu, S.; Wu, X.; Chi, Y.; Yan, J. Characterization of Tar Derived from Principal Components of Municipal Solid Waste. *Energy Fuels* **2015**, *29*, 7266−7274.
(7) Zhou, H.; Wu, C.; Onwudili, J. A.; Meng, A.; Zhang, Y.; Williams, P. T. Polycyclic Aromatic Hydrocarbons (PAH) Formation from the Pyrolysis of Different Municipal Solid Waste Fractions. *Waste Manage.* **2015**, *36*, 136−146.
(8) Ding, K.; Zhong, Z.; Zhong, D.; Zhang, B.; Qian, X. Pyrolysis of Municipal Solid Waste in a Fluidized Bed for Producing Valuable Pyrolytic Oils. *Clean Technol. Environ. Policy* **2016**, *18*, 1111−1121.
(9) Kunwar, B.; Cheng, H. N.; Chandrashekaran, S. R.; Sharma, B. K. Plastics to Fuel: A Review. *Renewable Sustainable Energy Rev.* **2016**, *54*, 421−428.
(10) Anuar Sharuddin, S. D.; Abnisa, F.; Wan Daud, W. M. A.; Aroua, M. K. A Review on Pyrolysis of Plastic Wastes. *Energy Convers. Manage.* **2016**, *115*, 308−326.
(11) McClelland, D. J.; Motagamwala, A. H.; Li, Y.; Rover, M. R.; Wittrig, A. M.; Wu, C.; Buchanan, J. S.; Brown, R. C.; Ralph, J.; Dumesic, J. A.; Huber, G. W. Functionality and Molecular Weight Distribution of Red Oak Lignin before and after Pyrolysis and Hydrogenation. *Green Chem.* **2017**, *19*, 1378−1389.
(12) Jarvis, J. M.; McKenna, A. M.; Hilten, R. N.; Das, K. C.; Rodgers, R. P.; Marshall, A. G. Characterization of Pine Pellet and Peanut Hull Pyrolysis Bio-Oils by Negative-Ion Electrospray

DOI: 10.1021/acs.energyfuels.8b00596
Energy Fuels 2018, 32, 7752−7761

Ionization Fourier Transform Ion Cyclotron Resonance Mass Spectrometry. *Energy Fuels* **2012**, *26*, 3810−3815.
(13) Sipilä, K.; Kuoppala, E.; Fagernäs, L.; Oasmaa, A. Characterization of Biomass-Based Flash Pyrolysis Oils. *Biomass Bioenergy* **1998**, *14* (2), 103−113.
(14) Oasmaa, A.; Kuoppala, E.; Solantausta, Y. Fast Pyrolysis of Forestry Residue. 2. Physicochemical Composition of Product Liquid. *Energy Fuels* **2003**, *17*, 433−443.
(15) Oasmaa, A.; Elliott, D. C.; Korhonen, J. Acidity of Biomass Fast Pyrolysis Bio-Oils. *Energy Fuels* **2010**, *24*, 6548−6554.
(16) Liu, Y.; Shi, Q.; Zhang, Y.; He, Y.; Chung, K. H.; Zhao, S.; Xu, C. Characterization of Red Pine Pyrolysis Bio-Oil by Gas Chromatography−Mass Spectrometry and Negative-Ion Electrospray Ionization Fourier Transform Ion Cyclotron Resonance Mass Spectrometry. *Energy Fuels* **2012**, *26* (7), 4532−4539.
(17) Oasmaa, A.; Kuoppala, E.; Gust, S.; Solantausta, Y. Fast Pyrolysis of Forestry Residue. 1. Effect of Extractives on Phase Separation of Pyrolysis Liquids. *Energy Fuels* **2003**, *17* (1), 1−12.
(18) Oasmaa, A.; Kuoppala, E. Fast Pyrolysis of Forestry Residue. 3. Storage Stability of Liquid Fuel. *Energy Fuels* **2003**, *17* (4), 1075−1084.
(19) Oasmaa, A.; Kuoppala, E.; Selin, J. F.; Gust, S.; Solantausta, Y. Fast Pyrolysis of Forestry Residue and Pine. 4. Improvement of the Product Quality by Solvent Addition. *Energy Fuels* **2004**, *18* (5), 1578−1583.
(20) Azargohar, R.; Jacobson, K. L.; Powell, E. E.; Dalai, A. K. Evaluation of Properties of Fast Pyrolysis Products Obtained, from Canadian Waste Biomass. *J. Anal. Appl. Pyrolysis* **2013**, *104*, 330−340.
(21) Vitasari, C. R.; Meindersma, G. W.; de Haan, A. B. Water Extraction of Pyrolysis Oil: The First Step for the Recovery of Renewable Chemicals. *Bioresour. Technol.* **2011**, *102*, 7204−7210.
(22) Fu, D.; Farag, S.; Chaouki, J.; Jessop, P. G. Extraction of Phenols from Lignin Microwave-Pyrolysis Oil Using a Switchable Hydrophilicity Solvent. *Bioresour. Technol.* **2014**, *154*, 101−108.
(23) Klein, G. C.; Angström, A.; Rodgers, R. P.; Marshall, A. G. Use of Saturates/Aromatics/Resins/Asphaltenes (SARA) Fractionation To Determine Matrix Effects in Crude Oil Analysis by Electrospray Ionization Fourier Transform Ion Cyclotron Resonance Mass Spectrometry. *Energy Fuels* **2006**, *20*, 668−672.
(24) Pütün, A. E.; Özcan, A.; Pütün, E. Pyrolysis of Hazelnut Shells in a Fixed-Bed Tubular Reactor: Yields and Structural Analysis of Bio-Oil. *J. Anal. Appl. Pyrolysis* **1999**, *52*, 33−49.
(25) Pütün, A. E.; Apaydm, E.; Pütün, E. Rice Straw as a Bio-Oil Source via Pyrolysis and Steam Pyrolysis. *Energy* **2004**, *29*, 2171−2180.
(26) Toraman, H. E.; Dijkmans, T.; Djokic, M. R.; Van Geem, K. M.; Marin, G. B. Detailed Compositional Characterization of Plastic Waste Pyrolysis Oil by Comprehensive Two-Dimensional Gas-Chromatography Coupled to Multiple Detectors. *J. Chromatogr. A* **2014**, *1359*, 237−246.
(27) Capunitan, J. A.; Capareda, S. C. Characterization and Separation of Corn Stover Bio-Oil by Fractional Distillation. *Fuel* **2013**, *112*, 60−73.
(28) Eide, I.; Neverdal, G. Fingerprinting Bio-Oils from Lignocellulose and Comparison with Fossil Fuels. *Energy Fuels* **2014**, *28*, 2617−2623.
(29) Kalogiannis, K. G.; Stefanidis, S. D.; Michailof, C. M.; Lappas, A. A.; Sjöholm, E. Pyrolysis of Lignin with 2DGC Quantification of Lignin Oil: Effect of Lignin Type, Process Temperature and ZSM-5 in Situ Upgrading. *J. Anal. Appl. Pyrolysis* **2015**, *115*, 410−418.
(30) Heydariaraghi, M.; Ghorbanian, S.; Hallajisani, A.; Salehpour, A. Fuel Properties of the Oils Produced from the Pyrolysis of Commonly-Used Polymers: Effect of Fractionating Column. *J. Anal. Appl. Pyrolysis* **2016**, *121*, 307−317.
(31) Silva, R. V. S.; Tessarolo, N. S.; Pereira, V. B.; Ximenes, V. L.; Mendes, F. L.; de Almeida, M. B. B.; Azevedo, D. A. Quantification of Real Thermal, Catalytic, and Hydrodeoxygenated Bio-Oils via Comprehensive Two-Dimensional Gas Chromatography with Mass Spectrometry. *Talanta* **2017**, *164*, 626−635.
(32) Negahdar, L.; Gonzalez-Quiroga, A.; Otyuskaya, D.; Toraman, H. E.; Liu, L.; Jastrzebski, J. T. B. H.; Van Geem, K. M.; Marin, G. B.; Thybaut, J. W.; Weckhuysen, B. M. Characterization and Comparison of Fast Pyrolysis Bio-Oils from Pinewood, Rapeseed Cake, and Wheat Straw Using 13C NMR and Comprehensive GC × GC. *ACS Sustainable Chem. Eng.* **2016**, *4*, 4974−4985.
(33) Hassan, E. B.; Elsayed, I.; Eseyin, A. Production High Yields of Aromatic Hydrocarbons through Catalytic Fast Pyrolysis of Torrefied Wood and Polystyrene. *Fuel* **2016**, *174*, 317−324.
(34) Mante, O. D.; Dayton, D. C.; Soukri, M. Production and Distillative Recovery of Valuable Lignin-Derived Products from Biocrude. *RSC Adv.* **2016**, *6*, 94247−94255.
(35) Shashkov, M. V.; Sidelnikov, V. N. Separation of Phenol-Containing Pyrolysis Products Using Comprehensive Two-Dimensional Chromatography with Columns Based on Pyridinium Ionic Liquids. *J. Sep. Sci.* **2016**, *39* (19), 3754−3760.
(36) Zhang, B.; Zhong, Z.; Ding, K.; Song, Z. Production of Aromatic Hydrocarbons from Catalytic Co-Pyrolysis of Biomass and High Density Polyethylene: Analytical Py-GC/MS Study. *Fuel* **2015**, *139*, 622−628.
(37) Zhang, H.; Xiao, R.; Nie, J.; Jin, B.; Shao, S.; Xiao, G. Catalytic Pyrolysis of Black-Liquor Lignin by Co-Feeding with Different Plastics in a Fluidized Bed Reactor. *Bioresour. Technol.* **2015**, *192*, 68−74.
(38) Syamsiro, M.; Saptoadi, H.; Norsujianto, T.; Noviasri, P.; Cheng, S.; Alimuddin, Z.; Yoshikawa, K. Fuel Oil Production from Municipal Plastic Wastes in Sequential Pyrolysis and Catalytic Reforming Reactors. *Energy Procedia* **2014**, *47*, 180−188.
(39) Artetxe, M.; Lopez, G.; Amutio, M.; Elordi, G.; Bilbao, J.; Olazar, M. Cracking of High Density Polyethylene Pyrolysis Waxes on HZSM - 5 Catalysts of Different Acidity. *Ind. Eng. Chem. Res.* **2013**, *52*, 10637−10645.
(40) Sfetsas, T.; Michailof, C.; Lappas, A.; Li, Q.; Kneale, B. Qualitative and Quantitative Analysis of Pyrolysis Oil by Gas Chromatography with Flame Ionization Detection and Comprehensive Two-Dimensional Gas Chromatography with Time-of-Flight Mass Spectrometry. *J. Chromatogr. A* **2011**, *1218*, 3317−3325.
(41) Salehi, E.; Abedi, J.; Harding, T. Bio-Oil from Sawdust: Pyrolysis of Sawdust in a Fixed-Bed System. *Energy Fuels* **2009**, *23* (7), 3767−3772.
(42) Bhattacharya, P.; Steele, P. H.; Hassan, E. B. M.; Mitchell, B.; Ingram, L.; Pittman Jr, C. U. Wood/plastic Copyrolysis in an Auger Reactor: Chemical and Physical Analysis of the Products. *Fuel* **2009**, *88* (7), 1251−1260.
(43) Wang, S.; Gu, Y.; Liu, Q.; Yao, Y.; Guo, Z.; Luo, Z.; Cen, K. Separation of Bio-Oil by Molecular Distillation. *Fuel Process. Technol.* **2009**, *90* (5), 738−745.
(44) Demirbas, A. Pyrolysis of Municipal Plastic Wastes for Recovery of Gasoline-Range Hydrocarbons. *J. Anal. Appl. Pyrolysis* **2004**, *72*, 97−102.
(45) Singh, R. K.; Ruj, B. Time and Temperature Depended Fuel Gas Generation from Pyrolysis of Real World Municipal Plastic Waste. *Fuel* **2016**, *174*, 164−171.
(46) Smith, E. A.; Park, S.; Klein, A. T.; Lee, Y. J. Bio-Oil Analysis Using Negative Electrospray Ionization: Comparative Study of High Resolution Mass Spectrometers and Phenolic versus Sugaric Components. *Energy Fuels* **2012**, *26*, 3796−3802.
(47) Jarvis, J. M.; Page-dumroese, D. S.; Anderson, N. M.; Corilo, Y.; Rodgers, R. P. Characterization of Fast Pyrolysis Products Generated from Several Western USA Woody Species. *Energy Fuels* **2014**, *28*, 6438−6446.
(48) Smith, E. A.; Thompson, C.; Lee, Y. J. Petroleomic Characterization of Bio-Oil Aging Using Fourier-Transform Ion Cyclotron Resonance Mass Spectrometry. *Bull. Korean Chem. Soc.* **2014**, *35* (3), 811−814.
(49) Ware, R. L.; Rowland, S. M.; Rodgers, R. P.; Marshall, A. G. Advanced Chemical Characterization of Pyrolysis Oils from Landfill Waste, Recycled Plastics, and Forestry Residue. *Energy Fuels* **2017**, *31*, 8210−8216.

DOI: 10.1021/acs.energyfuels.8b00596
Energy Fuels 2018, 32, 7752−7761

(50) Corilo, Y. E. *PetroOrg Software*; Florida State University: Tallahassee, FL, 2017; http://software.petroorg.com.
(51) Kaiser, N. K.; Quinn, J. P.; Blakney, G. T.; Hendrickson, C. L.; Marshall, A. G. A Novel 9.4 T FTICR Mass Spectrometer with Improved Sensitivity, Mass Resolution, and Mass Range. *J. Am. Soc. Mass Spectrom.* **2011**, *22*, 1343−1351.
(52) Blakney, G. T.; Hendrickson, C. L.; Marshall, A. G. Predator Data Station: A Fast Data Acquisition System for Advanced FT-ICR MS Experiments. *Int. J. Mass Spectrom.* **2011**, *306*, 246−252.
(53) Marshall, A. G.; Hendrickson, C. L.; Jackson, G. S. Fourier Transform Ion Cyclotron Resonance Mass Spectrometry : A Primer. *Mass Spectrom. Rev.* **1998**, *17*, 1−35.
(54) Aguado, J.; Serrano, D. P.; San Miguel, G.; Castro, M. C.; Madrid, S. Feedstock Recycling of Polyethylene in a Two-Step Thermo-Catalytic Reaction System. *J. Anal. Appl. Pyrolysis* **2007**, *79*, 415−423.
(55) Hsu, C. S.; Lobodin, V. V.; Rodgers, R. P.; McKenna, A. M.; Marshall, A. G. Compositional Boundaries for Fossil Hydrocarbons. *Energy Fuels* **2011**, *25*, 2174−2178.
(56) Lobodin, V. V.; Marshall, A. G.; Hsu, C. S. Compositional Space Boundaries for Organic Compounds. *Anal. Chem.* **2012**, *84*, 3410−3416.
(57) Cho, Y.; Birdwell, J. E.; Hur, M.; Lee, J.; Kim, B.; Kim, S. Extension of the Analytical Window for Characterizing Aromatic Compounds in Oils Using a Comprehensive Suite of High-Resolution Mass Spectrometry Techniques and Double Bond Equivalence versus Carbon Number Plot. *Energy Fuels* **2017**, *31*, 7874−7883.

DOI: 10.1021/acs.energyfuels.8b00596
Energy Fuels 2018, 32, 7752−7761